MOLECULAR AND CELLULAR BIOLOGY, May 2009, p. 2828–2840 Vol. 29, No. 10
0270-7306/09/$08.00+0 doi:10.1128/MCB.01830-08

H2AX Is Required for Cell Cycle Arrest via the p53/p21 Pathway▽†

Michalis Fragkos, Jaana Jurvansuu,‡ and Peter Beard*

Ecole Polytechnique Federale de Lausanne, Faculty of Life Sciences, Swiss Institute for Experimental Cancer Research (ISREC), 1015 Lausanne, Switzerland

Received 2 December 2008/Returned for modification 15 January 2009/Accepted 26 February 2009

Phosphorylation of H2AX (γH2AX) is an early sign of DNA damage induced by replication stalling. However, the role of H2AX in the repair of this type of DNA damage is still unclear. In this study, we used an inactivated adeno-associated virus (AAV) to induce a stalled replication fork signal and investigate the function of γH2AX. The cellular response to AAV provides a unique model to study γH2AX function, because the infection causes pannuclear H2AX phosphorylation without any signs of damage to the host genome. We found that pannuclear γH2AX formation is a result of ATR overactivation and diffusion but is independent of ATM. The inhibition of H2AX with RNA interference or the use of H2AX-deficient cells showed that γH2AX is dispensable for the formation and maintenance of DNA repair foci induced by stalled replication. However, in the absence of H2AX, the AAV-containing cells showed proteosome-dependent degradation of p21, followed by caspase-dependent mitotic catastrophe. In contrast, H2AX-proficient cells as well as H2AX-complemented $H2AX^{-/-}$ cells reacted by increasing p21 levels and arresting the cell cycle. The results establish a new role for H2AX in the p53/p21 pathway and indicate that H2AX is required for p21-induced cell cycle arrest after replication stalling.

The cellular response to DNA damage involves a series of events that lead to either cell cycle arrest or apoptosis. One of these events is the phosphorylation of histone 2AX (H2AX), which constitutes a significant portion (2 to 25%) of H2A (21). H2AX phosphorylation at serine 139 (γ-H2AX) was first identified in mammalian cells treated with ionizing irradiation and was found to be dependent on ataxia telangiectasia-mutated (ATM) kinase (21, 42). It was localized to irradiation-induced double-stranded DNA breaks, extending about 2 megabases around the breaks (41, 42). This type of response is conserved across species from humans to yeast (17, 40). Phosphorylation of H2AX takes place immediately after the generation of a DNA break and mediates the formation of clusters of proteins at the site of damage, called DNA damage response foci (19). The formation of γ-H2AX foci has also been shown after replication stalling and single-stranded DNA breaks (24, 39, 55). In that case, the phosphorylation of H2AX is dependent on ATM- and Rad3-related (ATR) kinase (12, 55) and not ATM.

The biological importance of H2AX phosphorylation was revealed by the H2AX knockout mouse, which was found to be growth retarded, immunodeficient, and moderately radiation sensitive (15). That study indicated a role of H2AX phosphorylation in various processes including cell growth, variable-diversity-joining recombination, and meiosis (21). Furthermore, H2AX-deficient embryonic stem cells were also genetically unstable, whereas H2AX haploinsufficiency was shown to contribute to genomic instability (5, 13). Although H2AX was initially thought to be required for recruiting DNA repair proteins to DNA damage response foci, it was later proven to be dispensable for attracting repair factors into foci, indicating that it is not necessary in the initial steps of the DNA damage response (14, 37). H2AX phosphorylation has also been shown to be dispensable in other cases of DNA repair, such as in retroviral postintegration DNA rejoining or in replication protein A (RPA) focus formation after replication stress (16, 33). On the other hand, γ-H2AX has been shown to be essential for concentrating repair proteins and maintaining the integrity of the DNA damage response foci (14). The role of γ-H2AX foci in the DNA damage signaling pathway induced by double-strand breaks is to act as docking areas for the recruitment of repair factors and to bring the broken DNA ends closer so that DNA repair is accomplished (4, 51). This model has recently been supported by a study showing that H2AX deficiency can lead to chromosome instability and cancer (23). Finally, the significance of H2AX in cell cycle arrest was previously demonstrated by Fernandez-Capetillo et al. (20) in a study where H2AX-null cells were defective in arresting at the G_2-M boundary after low-dose ionizing radiation. On the other hand, the role of H2AX in the damage response induced by stalled replication forks has not yet been clarified.

The response to DNA damage results in either cell cycle arrest, to allow the lesions to be repaired, or apoptosis. p53 is essential in both pathways. Specifically, in cell cycle arrest at G_1 phase, p53 enhances p21 transcription, which in turn inhibits cyclin-dependent kinase (cdk) activity. This prevents pRb from derepressing E2F1, inhibiting progression from G_1 to S phase (3, 28). Another way in which p21 leads to G_1 arrest is by binding to proliferating cell nuclear antigen (PCNA) and inhibiting its function in replication (35). The loss of p21 results in replication defects and may lead to cell death after treatment with anticancer drugs (26, 32). Progression to S phase after p53/p21-mediated arrest is achieved by the proteosome-dependent degradation of p21 (27).The p53/p21 pathway

* Corresponding author. Mailing address: EPFL, SV-ISREC, SV-1532, Station 19, 1015 Lausanne, Switzerland. Phone: 41-21-693 07 31. Fax: 41-21-693 07 20. E-mail: Peter.Beard@epfl.ch.

† Supplemental material for this article may be found at http://mcb.asm.org/.

‡ Present address: Structural Biology and Biophysics, Institute of Biotechnology, University of Helsinki, FIN-00014 Helsinki, Finland.

▽ Published ahead of print on 9 March 2009.

can also lead to G_2 arrest, preventing cells with damaged DNA from entering mitosis (11, 50). Cells may proceed to mitosis again by the degradation of p21 (2). The mechanism of p21 degradation has been controversial, with some reports claiming that it is ubiquitin dependent and some others showing the opposite (10, 44). Although the increase in p21 levels is a well-established pathway in DNA repair, a previous report by Bendjennat et al. (7) showed that p21 is degraded after low-dose UV irradiation. This response was shown to be essential for effective DNA repair through PCNA binding to chromatin. Recent studies further support the existence of this new pathway of DNA repair that involves the degradation of p21 (34, 47).

Viral infection can lead to a DNA damage response, which could be either beneficial or detrimental to the life cycle of the virus. An example of such a virus is adeno-associated virus (AAV), which has been shown to affect the host cell cycle and induce a significant DNA damage response (9, 30, 56). AAV is a defective virus whose replication depends on the presence of a helper virus such as adenovirus or herpesvirus (8). It belongs to the family *Parvoviridae* and has a 4.7-kb genome that encodes Rep and Cap polypeptides. The DNA of AAV has a single-stranded backbone flanked by two inverted terminal repeats that have a characteristic hairpin structure (8).

We have previously shown that irradiation of AAV with UV light to inactivate its genes and subsequent infection in the absence of helper virus lead to a significant DNA damage response, which resembles that provoked by chemically induced stalled replication forks (30). Moreover, in p53-deficient cells, AAV infection can result in cell death via mitotic catastrophe (29, 38). The AAV-induced DNA damage response is characterized by cell cycle arrest and an increase in p53 and p21 levels (38). The cell cycle arrest is dependent on ATR and subsequent Chk1 phosphorylation. Another characteristic of AAV-induced DNA damage signaling is the formation of DNA repair foci that include AAV DNA localized with replication proteins (RPA and DNA polymerase δ) and ATR, indicating that the response induced by the virus is due to stalled AAV replication (22, 30).

In this study, we investigated the role of H2AX phosphorylation in the DNA damage response induced by stalled replication forks. This was done by infecting cells with the replication-defective virus AAV. We discovered that H2AX is massively phosphorylated after AAV infection, leading to a pannuclear staining pattern. γ-H2AX staining was not attributable to host DNA damage, as the host genome was found to be intact. The response was rather a result of overactivated ATR, which is involved in the AAV-induced DNA damage response. H2AX phosphorylation was found to be dispensable for the initial steps of this signaling pathway but was shown to be required for the p53/p21 pathway to maintain p21 levels, leading to cell cycle arrest.

MATERIALS AND METHODS

Cell lines and chemicals. All cell lines were maintained in Dulbecco's modified Eagle's medium supplemented with 10% fetal bovine serum, penicillin-streptomycin, and ciprofloxacin (Ciproxin; Bayer). HeLa cells were used for the production of virus. GK41 kinase-dead ATR-inducible U2OS cells were described previously by Nghiem et al. (36). AT22IJE-T cells were described previously by Ziv et al. (58). H2AX-deficient ($H2AX^{-/-}$) and H2AX-proficient ($H2AX^{+/+}$) immortalized mouse embryonic fibroblasts (MEFs) were a kind gift from A. Nussenzweig. CsCl (used at a concentration of 3.5 mM) was obtained from Boehringer, dimethyl sulfoxide (DMSO) was obtained from Applichem, and DNase I (used at a concentration of 0.5 U/μl) was obtained from Roche. All other chemicals were purchased from Sigma. Doxorubicin was used at a concentration of 50 nM, and UCN01 was used at a concentration of 300 nM.

Virus production and infections. The production of AAV was previously described (57). All experiments were performed using UV-inactivated AAV2 unless otherwise stated. UV treatment of virus was used to inactivate the viral genes. In brief, virus samples were diluted in 50 μl of phosphate-buffered saline (PBS) and then UV inactivated on an empty tissue culture dish using a UV Stratalinker 2400 apparatus (Stratagene) at 240 mJ/cm^2. Virus samples were then used to infect cells in a small quantity of plain Dulbecco's modified Eagle's medium for 3 to 5 h. Complete medium was finally added to the cells. All AAV infections were performed at a multiplicity of infection of 10,000 unless otherwise stated.

Immunofluorescence staining and microscopy. Cells were plated onto fibronectin-treated coverslips 1 day before treatment. They were fixed with 5% formaldehyde for 10 min and then washed with PBS. Samples were blocked (0.5% NP-40, 5% milk powder, 1% fetal bovine serum) for 30 min. After being washed once with PBS, cells were incubated with primary antibodies for 45 to 60 min. Coverslips were washed with PBS and then incubated with secondary antibodies for another 45 to 60 min. They were then washed with PBS and stained with 0.1 μg/ml DAPI (4′,6′-diamidino-2-phenylindole) for 45 s. Finally, they were washed with PBS and distilled water and mounted onto diazabicyclooctane-glycerol (50%). For bromodeoxyuridine (BrdU) staining, cells were permeabilized using 0.5% Triton X-100, blocked in 2% bovine serum albumin solution, and stained with a BrdU-fluorescein isothiocyanate (FITC) antibody for 2.5 h.

The primary antibodies used were as follows: anti-α-tubulin (catalog number Ab7292; Abcam), anti-BrdU-FITC (347583; BD), anti-green fluorescent protein (GFP) (13970; Abcam), anti-H2AX (A300-082A; Bethyl), anti-γH2AX Ser139 (JBW301; Upstate Cell Signaling), and anti-phospho-RPA32 S4/S8 (05-636; Bethyl). The secondary antibodies used were Alexafluor-488, Alexafluor-568 (Molecular probes), and Cy3 (Jackson Immunoresearch) immunoglobulin G conjugates. Images were obtained using a Zeiss Axioplan microscope and were acquired with a Zeiss AxioCam MRm camera using Axiovision 4.5 software. The 63× (Plan-Apo/1.4 numerical aperture, oil) objective was used unless otherwise stated (10× [Plan-Neo/0.3 numerical aperture] or 20× [Plan-Apo/0.75 numerical aperture] objective). For live imaging, the Zeiss time-lapse Axiovert 100 microscope was used.

β-Galactosidase staining. Cells were fixed as described above. Samples were then blocked in 1% gelatin (dissolved in Tris-buffered saline [TBS]-Tween) by incubation at room temperature for 30 min. Cells were washed twice with TBS and then incubated with AAV capsid antibody (A20; Progen), diluted in TBS-Tween, for 60 min. Cells were washed three times with TBS-Tween and then incubated with β-galactosidase-conjugated secondary antibody (401607; Calbiochem) for 60 min. Samples were then washed three times with TBS-Tween and incubated in developing solution (0.2 mg/ml X-gal [5-bromo-4-chloro-3-indolyl-β-D-galactopyranoside], 5 mM $MgCl_2$, and 0.3 mg/ml Nitro Blue Tetrazolium dissolved in TBS) for 30 min at 37°C. Cells were washed twice with TBS-Tween and were then analyzed under a Leica DMIRB DC200 microscope using a 20× N-Plan/0.4-numerical-aperture objective, a Leica DFC340Fx camera, and Leica Application suite software.

Western blotting. Cell pellets were resuspended in 2.5 volumes of reporter lysis buffer (Promega) supplemented with a cocktail of protease inhibitors (Calbiochem). Samples were incubated on ice for 30 min and centrifuged at 16,000 × *g* for 20 min (4°C), and supernatants were then collected. The protein samples used in the H2AX Western blots were extracted by using NETN buffer (150 mM NaCl, 1 mM EDTA, 20 mM Tris [pH 8.0], 0.5% NP-40, protease inhibitors) and dissolving the protein pellets in 0.1 M HCl. Protein concentrations were calculated using the Bradford method (Bio-Rad), and 40 to 60 μg of protein samples was then separated on a sodium dodecyl sulfate-polyacrylamide gel (10% to 15%). The protein samples were transferred (semidry transfer) from the gel onto a nitrocellulose membrane (Bio-Rad), which was then blocked overnight at 4°C in blocking solution (5% milk powder in PBS–0.1% Tween). The membrane was incubated with primary antibodies for 1 h, washed with PBS-Tween, incubated with secondary antibodies for 1 h, and finally washed with PBS-Tween. The blots were visualized using the ECL assay (Amersham) according to the manufacturer's instructions.

The primary antibodies used were as follows: anti-α-tubulin (Ab7292; Abcam), anti-Chk1 (Ab22610; Abcam), anti-H2AX (A300-082; Bethyl), anti-γH2AX Ser139 (JBW301; Upstate Cell Signaling), anti-Flag M2 (F-3165; Sigma), anti-

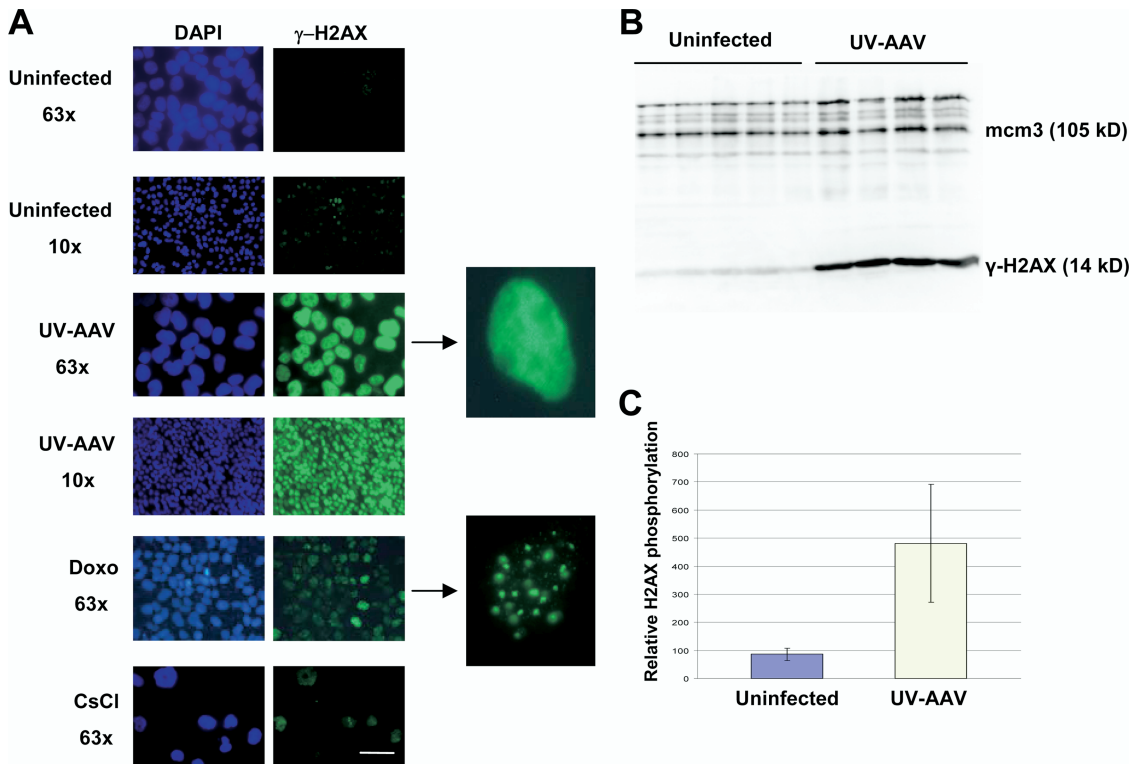

FIG. 1. AAV infection causes massive pannuclear phosphorylation of H2AX. (A) U2OS cells were infected with UV-inactivated AAV and then immunostained for γ-H2AX 1 day postinfection. Infected cells show a pannuclear staining pattern that is different from the one observed in doxorubicin (Doxo)-treated cells, which show foci of γ-H2AX (compare magnified images). Mock-infected cells were used as controls (CsCl). The bar corresponds to 35 μm for the 63× images and 225 μm for the 10× images. (B) Cells were infected with UV-AAV in several independent experiments and used to assay the levels of H2AX phosphorylation by Western blotting. Infection resulted in a massive phosphorylation of H2AX in host cells 1 day after infection. Mcm3 (minichromosome maintenance protein 3) was used as a loading control. (C) The levels of H2AX phosphorylation from these independent experiments were quantified, and means were compared. The difference between infected and uninfected cells is significant at a P value of 0.0038 (two-tailed t test).

GFP (11814460001; Roche), anti-Mcm3 (ab-4460; Abcam), anti-p21 (sc397; Santa Cruz), and anti-p53 (DO-12; Novocastra). Horseradish peroxidase-conjugated immunoglobulin G antibodies were used as secondary antibodies (Jackson Immunoresearch).

TUNEL and comet assays. The fluorescein FragEL DNA fragmentation detection kit (Calbiochem) was used to assay for the presence of double-stranded DNA breaks (terminal deoxynucleotidyltransferase-mediated dUTP-biotin nick end labeling [TUNEL] assay). The protocol was followed according to the manufacturer's instructions.

For the alkaline comet assay, the comet assay method from Trevigen was used according to the instructions provided by the manufacturer.

Propidium iodide staining and FACS analysis. The procedure for propidium iodide staining and fluorescence-activated cell sorter (FACS) analysis was described previously (22). Stained samples were analyzed using a Becton-Dickinson flow cytometer.

BrdU staining and FACS analysis. Cells were incubated with 10 μM BrdU for 40 min prior to FACS analysis. They were then washed once with PBS and processed according to the BD Pharmingen protocol (BrdU Flow kit, catalog number 559619). In brief, cells were fixed, permeabilized, refixed, and then treated with DNase. Cells were finally stained with BrdU-FITC antibody and 7-aminoactinomycin D.

H2AX RNA interference. Inhibition of H2AX was performed by transfecting cells with a short interfering RNA (siRNA) oligonucleotide (CAA CAA GAA GAC GCG AAU CdTdT) against H2AX. As a control, an siRNA oligonucleotide against GFP was used. Oligonucleotides were obtained by Dharmacon Research and were transfected using the Lipofectamine 2000 kit (Invitrogen).

Transfections. Transfections were performed using Lipofectamine 2000 reagent (Invitrogen) according to the manufacturer's instructions.

RESULTS

AAV induces massive pannuclear H2AX phosphorylation. We have previously shown that infection of p53-deficient cells with AAV can lead to cell death (38). This has been attributed to the ability of this virus to induce a DNA damage response that is dependent on the formation of stalled replication forks on AAV origins of replication (22, 30). In those experiments, as well as in the experiments described in this study, AAV was UV treated in order to prevent the expression of the viral genes. Further investigation of the DNA damage response induced by the UV-inactivated AAV (UV-AAV) led to the observation that infected U2OS cells induce massive phosphorylation of H2AX (Fig. 1). This phenomenon was also observed in an array of cell lines other than U2OS (see Fig. S1 in the supplemental material).

This result was unexpected, since UV-treated AAV is not capable of integrating into the host cell's genome. Furthermore, AAV has never been shown to have histone molecules within its capsid (8). The γ-H2AX staining pattern observed in AAV-infected cells is also remarkably distinct from that of cells treated with DNA-damaging agents such as doxorubicin. AAV-infected cells showed pannuclear H2AX phosphorylation, whereas doxorubicin-treated cells induced foci of γ-H2AX (Fig. 1A). It should

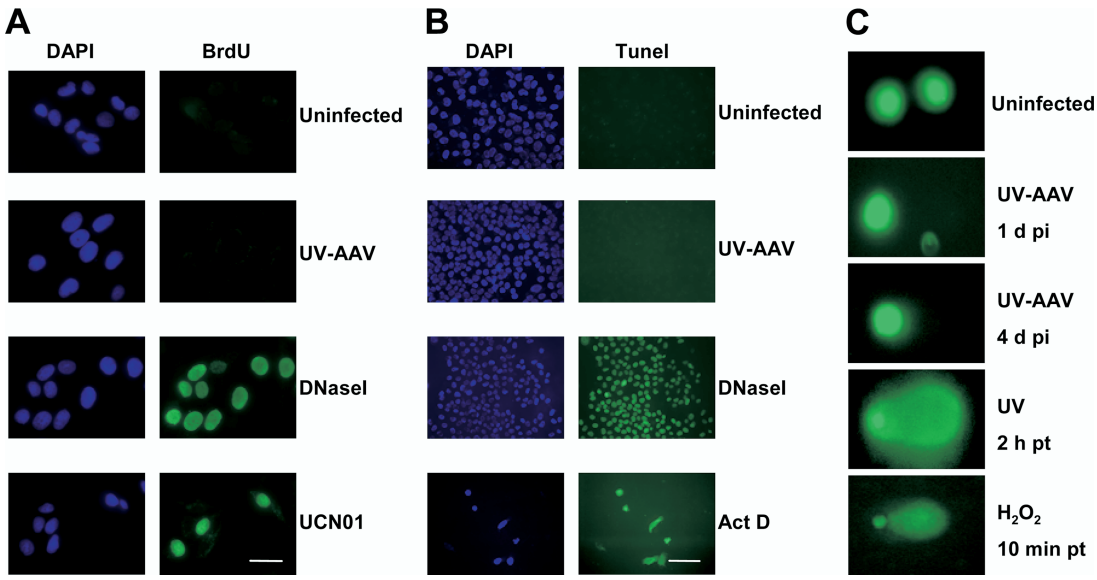

FIG. 2. AAV infection does not affect the stability of the host genome. (A) U2OS cells were pretreated for 24 h with BrdU (3.3 μM) and then immunostained for BrdU without denaturation. UV-AAV-infected cells did not stain positive, whereas the DNase I-treated and some of the UCN01-treated cells stained positive for BrdU. All stainings were performed 1 day after treatment. Bar, 30 μm. (B) TUNEL assay showing that AAV-infected cells do not contain DNA breaks. Actinomycin D (ActD) (1 μg/ml) and DNase I-treated cells were used as controls. Images were obtained using the 20× objective. Bar, 100 μm. (C) Comet assay showing an absence of DNA damage in infected U2OS cells. UV (50 mJ/cm^2)- and H_2O_2 (100 μM)-treated cells were used as controls. pi, postinfection; pt, posttreatment.

also be noted that in contrast to the doxorubicin-induced γ-H2AX foci, AAV-induced pannuclear H2AX phosphorylation was not established immediately but about 6 h after infection (see Fig. S2 in the supplemental material). The induction of H2AX phosphorylation was not caused by CsCl, which is used during viral production (Fig. 1A). The quantity of H2AX phosphorylation was measured in infected U2OS cells by protein extraction and Western analysis (Fig. 1B). The results were quantified and are presented in Fig. 1C. It is evident that the cells infected with AAV induce H2AX phosphorylation that is significantly stronger than that of uninfected cells.

AAV induces a DNA damage response without damaging the host genome. Pannuclear AAV-induced H2AX phosphorylation could be a result of genome-wide DNA damage in the host cell. AAV could potentially induce increased initiation of replication in the host genome, which could in turn produce DNA breaks and therefore H2AX phosphorylation. To test this, U2OS cells were pretreated with BrdU and then infected with UV-AAV. Cells were assayed for BrdU incorporation by staining in the absence of denaturation so as to identify single-strand DNA breaks. The experiment showed no signs of single-strand DNA breaks that would correlate with an increased presence of cellular stalled replication forks (Fig. 2A). Cells treated with UCN01, which is an inhibitor of Chk1, were used as a control, as it has been shown that Chk1 inhibition leads to an increased initiation of replication origins and therefore single-strand DNA breaks (49). DNase I-treated cells were also used as a positive control.

The induction of double-strand DNA breaks after infection with AAV was assayed by performing a TUNEL assay. U2OS cells were infected with UV-AAV and then tested for DNA breaks. As can been seen in Fig. 2B, this assay confirmed the absence of DNA breaks in the genome of the AAV-infected cells, indicating that H2AX phosphorylation is not a result of cellular double-strand DNA breaks. Treatment with actinomycin D as a control led to significant levels of apoptosis-related DNA fragmentation, which also resulted in reduced cell density in the sample. DNase I-treated cells served as another positive control.

The induction of DNA breaks after AAV infection was also assayed by performing an alkaline comet assay. As shown in Fig. 2C, UV-AAV-infected U2OS cells did not show comet tails. On the other hand, when cells were treated with UV or H_2O_2, which damage cellular DNA, they showed clear tails indicative of significant DNA damage. Altogether, our data suggest that a DNA damage response can be evoked without the presence of genomic DNA lesions. Accumulation of DNA damage response proteins on the AAV genome is sufficient to initiate DNA damage signaling, as seen with H2AX phosphorylation.

AAV-induced phosphorylation of H2AX is dependent on ATR and not ATM. The next step in our study was to investigate the mechanism of H2AX phosphorylation after infection with AAV. The induction of γ-H2AX foci after formation of stalled replication forks is a result of phosphorylation by ATR kinase (12, 55). In order to investigate whether the formation of stalled replication forks on the AAV genome would activate ATR, which in turn would phosphorylate the host's H2AX, AAV-infected U2OS cells were treated with caffeine, which is known to inhibit ATR and ATM kinases (43). Caffeine treatment inhibited the pannuclear type of H2AX phosphorylation, indicating that either ATR or ATM is involved in this type of response (Fig. 3A). To verify the effectiveness of caffeine treatment, infected U2OS cells were treated with caffeine, stained with propidium iodide and analyzed by FACS to investigate the cell cycle status of the cells (Fig. 3B). We have previously

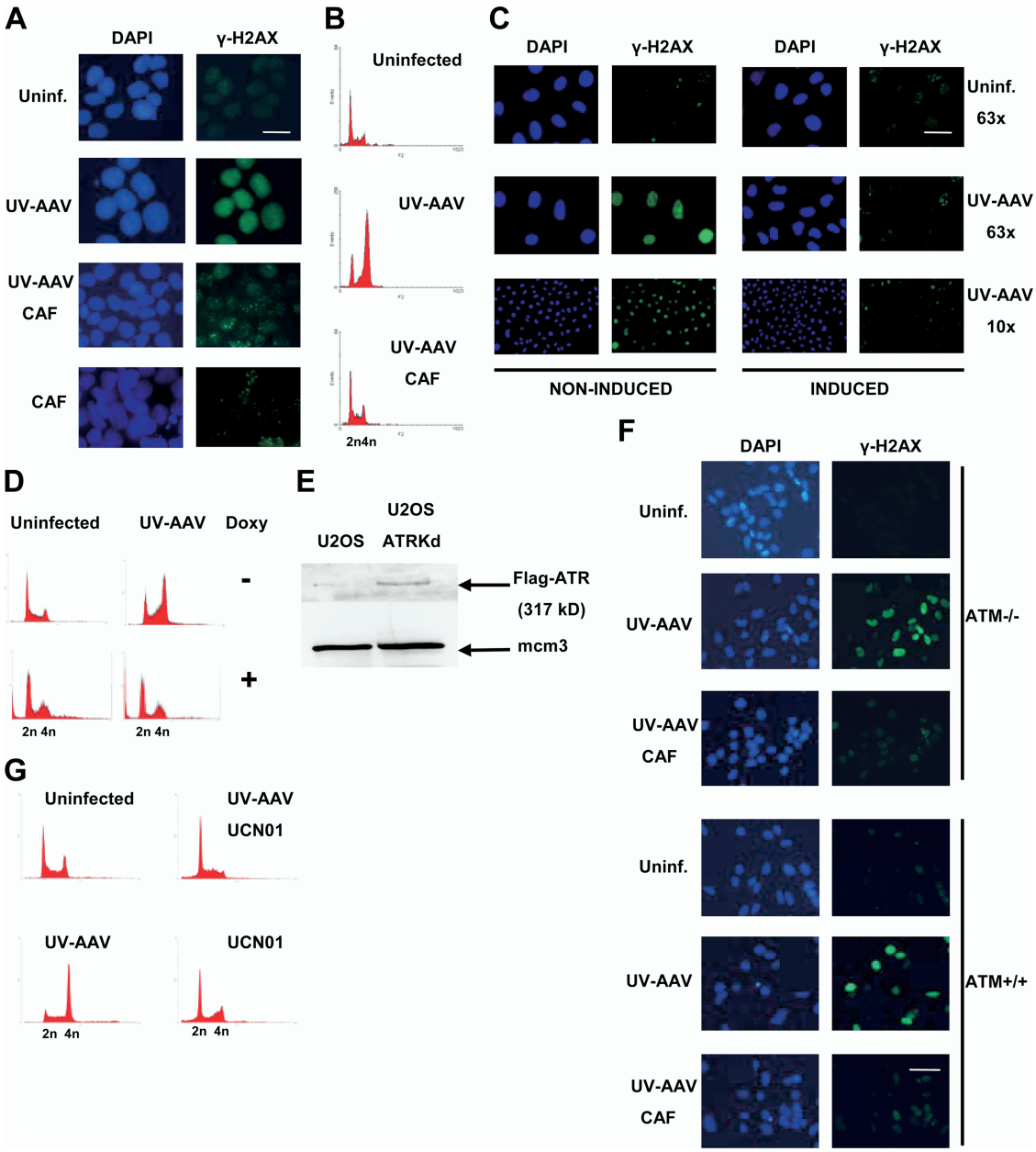

FIG. 3. AAV-induced H2AX phosphorylation is ATR dependent. (A) Caffeine (CAF) treatment inhibits the pannuclear phosphorylation of H2AX. AAV-infected U2OS cells were treated with caffeine at 3 mM and showed an absence of pannuclear γ-H2AX staining 1 day postinfection. Some cells showed background focal staining of γ-H2AX similar to that often observed in untreated U2OS cells. Cells were also treated with caffeine alone, which did not have an effect on H2AX. Bar, 20 μm. (B) FACS analysis to test the effectiveness of caffeine treatment. Infected cells were treated with caffeine, which inhibited AAV-induced cell cycle arrest. (C) GK41 (kinase-dead ATR-inducible U2OS) cells were induced with doxycycline (Doxy) for 2 days, infected, and then maintained in doxycycline-containing medium. Cells were analyzed by immunostaining 1 day after infection. Bars, 35 μm (63×) and 130 μm (10×). (D) The effectiveness of doxycycline was confirmed by analyzing the cell cycle status of cells by FACS. (E) Expression of Flag-tagged kinase-dead ATR in doxycycline-induced GK41 cells was confirmed by Western blotting. Mcm3 was used as a loading control. (F) Immunostaining showing that ATM-deficient cells are capable of inducing H2AX phosphorylation after UV-AAV infection. AT22IJE-T cells were infected, treated or not with caffeine, and stained 1 day postinfection. $ATM^{+/+}$ cells were used as a control. Bar, 35 μm. (G) Cell cycle analysis of AAV-infected and chk1-inhibited (UCN01) U2OS cells. Cells treated with UCN01 alone were used as controls. Uninf., uninfected.

shown that infection with UV-AAV leads to cell cycle arrest at G_2 phase that is dependent on ATR (38). As shown in Fig. 3B, caffeine prevented U2OS-infected cells from arresting at G_2 phase, indicating that caffeine treatment was indeed effective.

The involvement of ATR in AAV-induced H2AX phosphorylation was further studied by using the GK41 cell line, which expresses an inducible Flag-tagged kinase-dead version of ATR that functions in a dominant-negative way to inactivate the endogenous functional protein. Noninduced cells showed pannuclear phosphorylation of H2AX after AAV infection,

whereas induced cells overexpressing the kinase-dead ATR did not exhibit significant levels of γ-H2AX staining (Fig. 3C). This experiment suggests that AAV-induced H2AX phosphorylation is ATR dependent. A control FACS analysis was then performed using propidium iodide-stained AAV-infected GK41 cells and showed that these cells do not arrest at G_2 phase after induction with doxycycline (Fig. 3D). This indicates that doxycycline induction functions properly, leading to an overexpression of the kinase-dead ATR. A control Western blot was also performed to confirm the expression of the Flag tagged-ATR mutant. GK41 cells were treated with doxycycline for 24 h and then used to extract protein. As can be seen in Fig. 3E, induction with doxycycline led to the expression of Flag-tagged kinase-dead ATR.

We next tested whether ATM is involved in AAV-induced pannuclear H2AX phosphorylation. In order to do this, AT22IJE-T/pEBS7 (ATM-deficient) cells were infected with UV-AAV, and the phosphorylation of H2AX was examined by immunofluorescence (Fig. 3F). ATM-null cells showed high levels of γ-H2AX staining, indicating that ATM is not responsible for this response. Treatment with caffeine, which inhibits ATR, abolished H2AX phosphorylation, supporting our previous conclusion that ATR is responsible for the AAV-induced phosphorylation of H2AX. The same experiment was performed using the ATM-proficient isogenic cell line AT22IJE-T/pEBS7-YZ5, which behaved the same as the ATM-deficient cell line.

To further test the activation of the ATR/Chk1 pathway after infection with AAV, cells were infected and at the same time treated with the Chk1 inhibitor UCN01. The cells were examined by flow cytometry 1 day postinfection and showed no G_2 arrest, indicating that Chk1 is indeed required for the signaling pathway induced by the virus (Fig. 3G). These data altogether suggest that AAV infection induces a pannuclear phosphorylation of H2AX that is dependent on the ATR/Chk1 pathway and not on ATM.

In order to investigate how ATR activation leads to this pannuclear type of H2AX phosphorylation, we examined the kinetics of the AAV-induced foci, which include ATR and RPA (30). Cells were transfected with a GFP-tagged RPA70 construct (33) and then infected with UV-AAV 24 h posttransfection. The cells were examined for GFP under a live-imaging microscope for 17 h by image acquisition every 5 min. The time-lapse video (see Fig. S3A in the supplemental material) indicates that the foci induced by UV-AAV do not move and remain relatively immobile in relation to each other. These data suggest that ATR could directly phosphorylate H2AX only if it diffuses away from these foci. The localization of the overexpressed GFP-RPA70 to the AAV-induced foci was confirmed by the experiment shown in Fig. S3B in the supplemental material. The mobility of H2AX was considered unlikely, as our previous work has shown that AAV-induced γ-H2AX is chromosome fixed rather than soluble (29).

H2AX is dispensable for the formation and maintenance of AAV-induced foci. We then asked whether phosphorylation of H2AX is required for the DNA damage signaling pathway induced by AAV. In order to test this, the production of H2AX was inhibited by using an siRNA molecule. U2OS cells were infected with UV-AAV and examined 4 days after infection to allow AAV-infected cells to enlarge (due to cell cycle arrest) and thus be distinguished from noninfected ones. The contribution of H2AX phosphorylation to AAV-induced DNA damage signaling was investigated by immunostaining for phospho-RPA32, which is localized in the AAV-induced foci (Fig. 4A). Depletion of H2AX was controlled by staining for γ-H2AX. Figure 4A indicates that AAV-infected cells (cells with enlarged nuclei) that do not exhibit H2AX phosphorylation (H2AX inhibition) do show DNA damage response foci. These data therefore suggest that H2AX phosphorylation induced by AAV is not required for the formation of DNA repair foci as well as for their maintenance 4 days after infection. siRNA-mediated H2AX inhibition was confirmed further by Western blotting (Fig. 4B).

An additional experiment was then performed to confirm the above-described conclusion. $H2AX^{-/-}$ MEFs were infected with UV-AAV and stained for phospho-RPA32 to identify the DNA damage response. As can be seen in Fig. 4C, H2AX-null cells are still able to induce a DNA damage response exhibited by the presence of phospho-RPA32 foci. The absence of H2AX expression in $H2AX^{-/-}$ MEFs was confirmed by Western blotting (Fig. 4D). In order to confirm that the foci observed in MEFs result from infection with the virus, we examined the infectivity of AAV in murine cells. Specifically, MEFs were infected with AAV and then stained for AAV capsid proteins using a β-galactosidase-conjugated antibody (Fig. 4E). Cells were examined under a bright-field microscope and showed high levels of infection comparable to those of human U2OS cells. These data together suggest that H2AX phosphorylation is dispensable for the initial step of the AAV-induced DNA damage signaling pathway, which involves the formation of DNA repair foci, and also for maintaining repair factors like RPA in these foci.

H2AX is required for p21-induced cell cycle arrest. We then examined the protein levels of a series of factors involved in the AAV-induced DNA damage response in $H2AX^{-/-}$ MEFs. Cells were infected with UV-AAV, and Western blotting for p21 and Chk1 was performed (Fig. 5A). An unexpected drop in the levels of p21 was observed in AAV-infected $H2AX^{-/-}$ cells. On the other hand, in $H2AX^{+/+}$ cells, p21 levels increased after infection. A loss of p21 was not observed in $H2AX^{-/-}$ cells treated with doxorubicin. The levels of Chk1 increased in both H2AX-deficient and $H2AX^{+/+}$ AAV-infected cells. We also examined the levels of p53 in AAV-infected $H2AX^{-/-}$ MEFs and found that the level of p53, unlike p21, was not diminished after infection with UV-AAV (Fig. 5B). In $H2AX^{+/+}$ MEFs as well as in U2OS cells, p53 levels increased after infection. These results indicate that the absence of H2AX leads to a decrease in p21 levels after AAV infection without any change in p53 levels.

We then examined whether the AAV-induced loss of p21 is proteosome dependent. AAV-infected $H2AX^{-/-}$ cells were treated with the proteosome inhibitor MG132, and p21 levels were assayed by Western blotting. As can be seen in Fig. 5C, MG132 prevented the loss of p21, supporting the idea that p21 levels drop after AAV infection due to proteosome-dependent degradation.

The cell cycle status of H2AX-deficient cells after infection with UV-AAV was then examined. Cells were stained with propidium iodide and analyzed by FACS analysis (Fig. 5D). Our results showed that infection with UV-AAV led to signif-

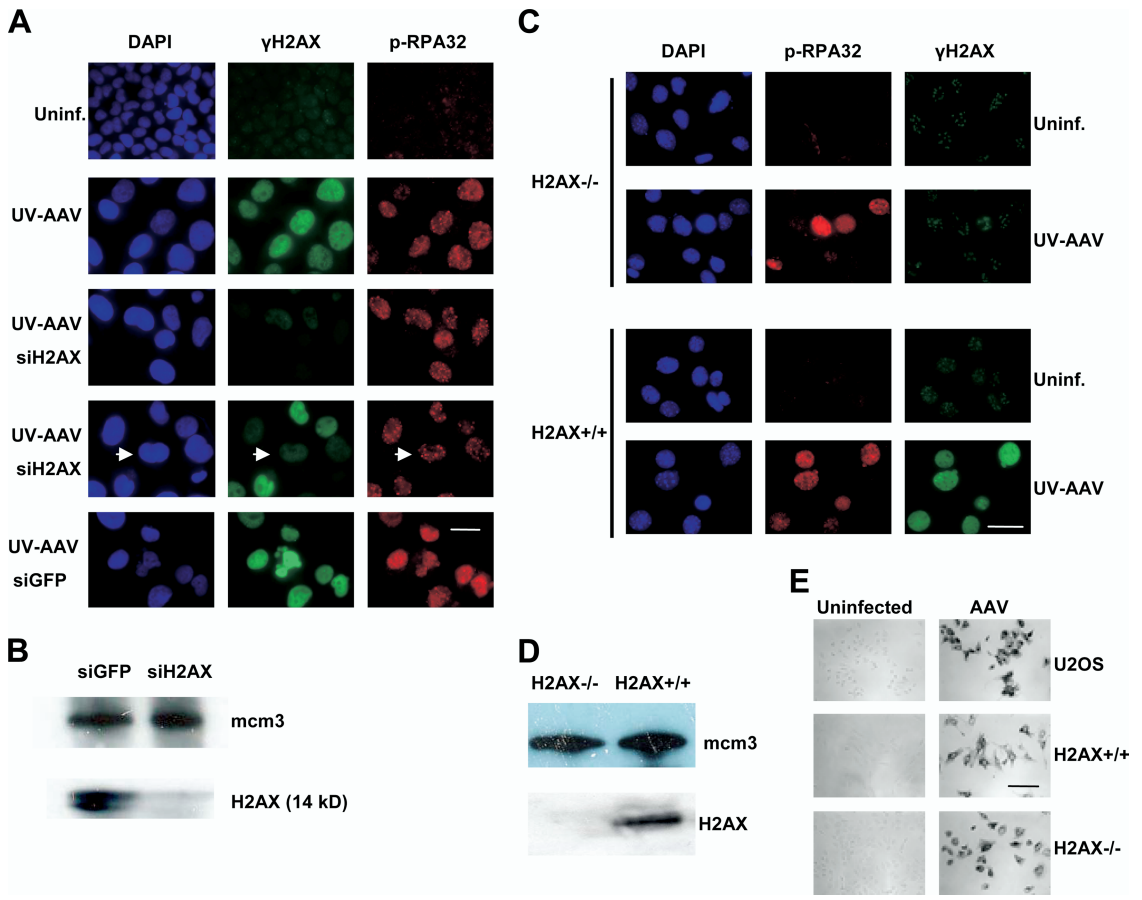

FIG. 4. H2AX phosphorylation is dispensable for formation and maintenance of AAV-induced foci. (A) Inhibition of H2AX by siRNA does not prevent formation of DNA damage response foci. Cells were transfected with an siRNA oligonucleotide against H2AX and infected with UV-AAV on the same day. Infected cells (with large DAPI-stained nuclei) with no γ-H2AX staining still form foci (phospho-RPA32 staining). An example of such a cell is indicated by arrows. Cells treated with GFP siRNA (siGFP) were used as a control. Bar, 30 μm. (B) Control Western blot showing the effectiveness of H2AX inhibition by siRNA. Uninf., uninfected. (C) Immunofluorescent staining showing that $H2AX^{-/-}$ MEFs form AAV-induced foci. MEFs were stained for γ-H2AX and phospho-RPA32 1 day after infection. $H2AX^{+/+}$ MEFs were used as a control. Bar, 40 μm. (D) Western blot to check that $H2AX^{-/-}$ cells do not express H2AX. Mcm3 was used as a loading control. (E) Control experiment to show that MEFs are infectible with AAV. Infected MEFs were immunostained with a β-galactosidase-conjugated AAV antibody 1 day postinfection and were compared to infected U2OS cells. Bar, 130 μm.

icant cell death (4 days postinfection). On the other hand, $H2AX^{+/+}$ cells did not show a change in their cell cycle status, with the majority of the cells being in G_1 phase. In both cell types, doxorubicin led to a strong cell cycle arrest at G_2 phase. In order to examine whether the G_1 peak seen in AAV-infected $H2AX^{+/+}$ cells corresponds to cell cycle arrest, $H2AX^{+/+}$ cells were either infected or treated with doxorubicin and examined by bright-field microscopy 4 days after treatment. As shown in Fig. 5E, it is clear that infection with UV-AAV inhibited cell division even more than doxorubicin that induces a G_2 arrest. To test whether this arrest reflects an activation of the G_1/S checkpoint, the cells were examined for BrdU incorporation by staining with a BrdU-FITC conjugate antibody and performing flow cytometry (Fig. 5F). In $H2AX^{+/+}$ MEFs, the population of cells in S phase (BrdU-positive cells) decreased sharply after infection. On the other hand, in $H2AX^{-/-}$ cells, infection resulted in a significant increase in the number of dead cells. Also taking into account that p21 and p53 levels increase after infection with UV-AAV in $H2AX^{+/+}$ cells (Fig. 5A and B), we can conclude that the G_1 peak seen in AAV-infected $H2AX^{+/+}$ cells (Fig. 5D) corresponds to cell cycle arrest.

To further investigate if the cell death seen in $H2AX^{-/-}$ MEFs is linked to the degradation of p21, H2AX-null cells were infected with UV-AAV and then treated with MG132. Cell cycle analysis was again performed by FACS and showed that the inhibition of the proteosome (and therefore of p21 degradation) prevented a significant portion of the cell population from undergoing cell death (Fig. 5G). This experiment was replicated, and the averages of data for the sub-G_1 populations are presented in Fig. 5H. Overall, these data suggest that H2AX is required for the p53/p21 pathway to function and leads to cell cycle arrest at G_1 phase. In the absence of H2AX, AAV infection leads to cell death that is likely attributable to the suppression of the G_1 checkpoint due to the degradation of p21.

In order to investigate this potential new role of H2AX further, a plasmid expressing GFP-tagged H2AX (45) was used

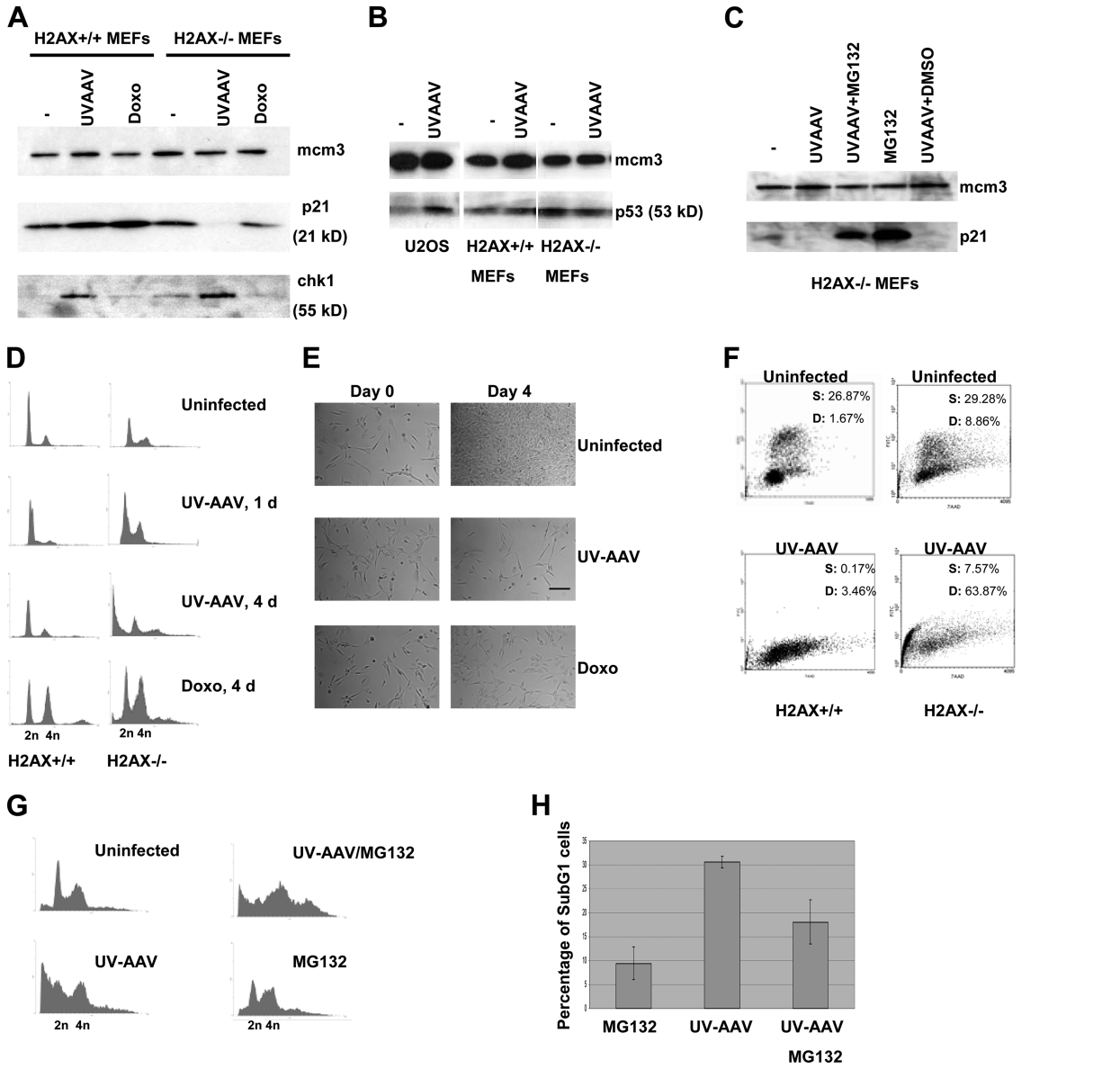

FIG. 5. H2AX phosphorylation is part of the p53/p21 pathway leading to cell cycle arrest. (A) Western blot showing loss of p21 and increase of Chk1 2 days after infection with UV-AAV in $H2AX^{-/-}$ cells but not after doxorubicin (Doxo) treatment. $H2AX^{+/+}$ cells were used as a control. Mcm3 was used as a loading control. (B) Western blot indicating that p53 levels remain unchanged after UV-AAV infection of $H2AX^{-/-}$ cells. In $H2AX^{+/+}$ cells, the levels of p53 increased after infection. U2OS cells were used as a control. (C) Loss of p21 in AAV-infected $H2AX^{-/-}$ cells is proteosome dependent. p21 levels were assayed by Western blotting of AAV-infected cells treated with the proteosome inhibitor MG132 (10 μM) 14 h before protein extraction. DMSO treatment was used as a control, as MG132 was diluted in DMSO. (D) FACS analysis showing that $H2AX^{-/-}$ cells die after infection with AAV. $H2AX^{+/+}$ cells did not have the same behavior. Doxorubicin resulted in cell cycle arrest at G_2 phase in both cell types tested. (E) Control experiment showing that AAV infection results in G_1 arrest in $H2AX^{+/+}$ cells. Cells were infected with UV-AAV, and bright-field images were taken 4 days after infection. Control uninfected cells were seen to be overgrown compared to the infected cells. Doxorubicin-treated cells were used as a control for cell cycle arrest. Bar, 55 μm. (F) FACS analysis of BrdU-stained MEFs. BrdU incorporation (FITC) (*y* axis) was measured against DNA content (7-aminoactinomycin D) (*x* axis). S, S-phase cells; D, dead cells. (G) Inhibition of the proteosome prevents AAV-induced cell death in $H2AX^{-/-}$ cells. AAV-infected cells were treated with MG132 and examined by FACS 2 days postinfection. Treatment with MG132 alone has little effect on the cell cycle in these cells. (H) The experiment described in G was replicated, and the average percentages of sub-G_1-phase populations were quantified. Error bars show standard deviations.

to transiently transfect H2AX-deficient MEFs. Figure 6A shows transfected $H2AX^{-/-}$ MEFs expressing H2AX and GFP. Such transfected cells were infected with UV-AAV on the same day as the transfection and were analyzed by propidium iodide staining and flow cytometry 4 days postinfection. Figure 6B shows the results of a typical experiment. The infected cells that had been previously transfected with the GFP-H2AX plasmid were protected from cell death, as only 16.3% of the total population was found in the sub-G_1 region, compared to 35.2% of the infected cells that had been transfected

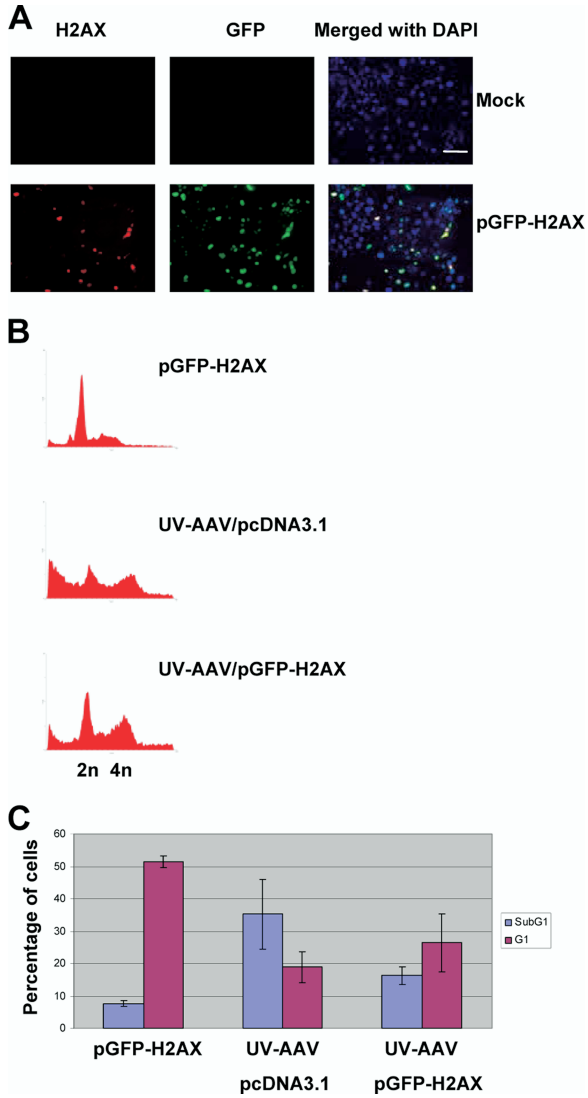

FIG. 6. H2AX rescues AAV-infected cells from cell death. (A) Control experiment to test the transfection efficiency of $H2AX^{-/-}$ MEFs. Cells were transfected with a GFP-H2AX-expressing plasmid and then immunostained for H2AX and GFP 2 days posttransfection. Bar, 180 μm. (B) Transient expression of H2AX prevents cell death and increases the 2n and 4n populations in AAV-infected $H2AX^{-/-}$ MEFs. Cells were transfected either with pGFP-H2AX or with an empty pcDNA3.1 vector (Invitrogen) and then infected with UV-AAV on the same day. The cell cycle status of the cells was analyzed by FACS 4 days after treatment. Transfection with pGFP-H2AX in noninfected cells did not have a significant effect. (C) Quantification of the sub-G_1 and G_1 populations in control-transfected (two replicates), the mock-transfected AAV-infected (three replicates), and the pGFP-H2AX-transfected AAV-infected (three replicates) $H2AX^{-/-}$ MEFs from the experiment described in the legend for panel B.

with an empty vector (Fig. 6C). In addition, the G_1 population of cells in the infected sample increased from 18.8% to 26.4% after the transient expression of H2AX.

p21 degradation was observed in $H2AX^{-/-}$ cells infected with UV-AAV but not in cells treated with doxorubicin. This result raised the question of whether this phenomenon is unique for the DNA damage response induced by AAV or if it can be a result of replication stress induced by other agents. To address this question, we treated H2AX-deficient cells with hydroxyurea (HU) or UV and examined the levels of p21 by Western blotting (Fig. 7A). In both cases, p21 levels did not increase, implying that the H2AX-null cells choose a pathway that does not involve p21 to respond to DNA damage. In particular, no p21 was observed after treatment with HU, whereas in the case of UV, the p21 levels remained relatively constant. On the other hand, $H2AX^{+/+}$ cells responded by increasing p21 levels after both treatments.

The role of H2AX in the p53/p21 pathway was also investigated by transiently transfecting H2AX-deficient MEFs with the GFP-tagged H2AX-expressing plasmid and examining the levels of p21 2 days after infection with UV-AAV or treatment with the indicated replication-blocking agents. As shown in Fig. 7B, the p21 levels in the cells expressing H2AX were higher than those of the nontransfected cells, indicating that H2AX is indeed part of the p53/p21 pathway. In conclusion, the absence of H2AX results in the activation of a DNA damage response pathway that is quantitatively and qualitatively different from the p53/p21 pathway and correlates with p21 degradation, leading to cell death.

H2AX-deficient cells die of caspase-dependent mitotic catastrophe. We then addressed the question of how $H2AX^{-/-}$ cells die after infection with UV-AAV. The cells were stained with DAPI 2 days after infection (Fig. 8A). This experiment showed that H2AX-null cells die by defective mitosis, since a large number of micronucleated cells was identified. This was observed neither in AAV-infected $H2AX^{+/+}$ cells nor in doxorubicin-treated cells. Mitotic catastrophe can be a result of the formation of multiple spindle poles. To test this, AAV-infected $H2AX^{-/-}$ cells were stained for α-tubulin and showed multiple spindle poles (Fig. 8B). Again, $H2AX^{+/+}$ cells as well as doxorubicin-treated MEFs did not show multiple spindle poles. These data indicate that H2AX-null MEFs die of mitotic catastrophe after infection with UV-AAV.

In order to examine whether an apoptotic pathway is involved in this type of cell killing, H2AX-deficient MEFs were infected and then treated with z-vad (carbobenzoxy-vanyl-alanyl-aspartyl-[*O*-methyl]-fluoromethyl-ketone), which is a pancaspase inhibitor. The cell cycle status of the cells was then examined by propidium iodide staining and flow cytometry. As shown in Fig. 8C, inhibition of caspase activity prevented a significant portion of cell death, indicating that AAV-infected H2AX-null cells die by mitotic failure that is dependent on caspases.

DISCUSSION

AAV induces pannuclear H2AX phosphorylation in the absence of cellular DNA lesions. Phosphorylation of H2AX is a nuclear marker of various types of DNA damage, ranging from double-strand DNA breaks to stalled replication forks. In this study, we show that H2AX becomes phosphorylated in the absence of cellular DNA damage. U2OS cells were infected with UV-inactivated AAV, which is known to initiate a DNA damage signaling pathway that involves ATR and Chk1 kinases and results from viral replication stalling. Although combinations of stimuli are possible, any contribution from inverted terminal repeat processing is apparently relatively minor, as shown in our previous studies (22, 30). Our data show that

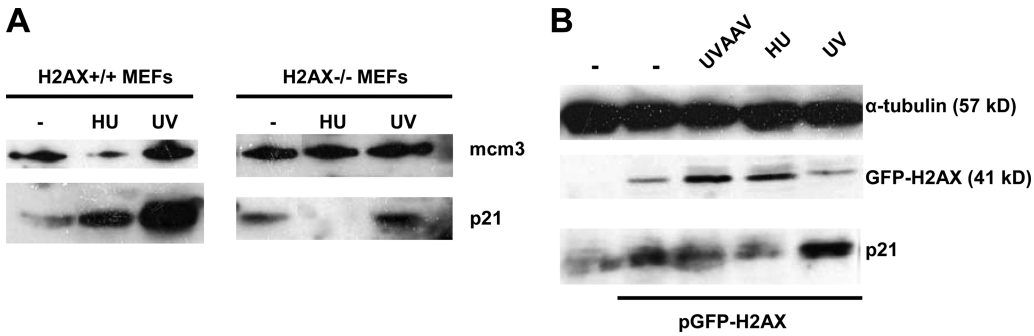

FIG. 7. p21 degradation in H2AX$^{-/-}$ cells treated with inducers of stalled replication. (A) Western blot indicating that p21 degradation is not observed only in the AAV-induced DNA damage response. H2AX$^{-/-}$ and H2AX$^{+/+}$ cells were treated with HU at 10 mM and UV at 100 J/m^2 and then assayed for p21 2 days posttreatment. p21 levels increased only in H2AX$^{+/+}$ cells. Mcm3 was used as a loading control. (B) Transfection with pGFP-H2AX prevents p21 degradation in H2AX$^{-/-}$ MEFs infected with UV-AAV or treated with replication-stalling agents. Cells were transiently transfected and treated with HU or UV or UV-AAV on the same day. GFP-tagged H2AX was detected using a GFP antibody, and α-tubulin was used as a loading control.

AAV infection does not damage the host genome or affect the host cell's replication. Nevertheless, it induces massive phosphorylation of H2AX in a pannuclear fashion. UV-inactivated AAV has persistent covalent intrastrand cross-links that do not allow the virus to integrate into the host genome (30). Moreover, AAV DNA foci are not associated with H2AX, and the UV-inactivated form of the virus was shown not to exist in concatameric forms that could potentially attract histone molecules (8, 30). We therefore conclude that AAV can initiate γH2AX signaling in the host cell through the accumulation of DNA damage response factors onto its genome and without damaging the cellular DNA.

Our data clearly support the notion that it is the accumulation and interaction of early sensors of DNA damage that are sufficient to cause DNA damage signaling, suggesting that cells respond to protein clusters of DNA repair factors rather than to cellular DNA damage itself. These results are consistent with a recent study showing that the binding of DNA repair factors to chromatin is enough to trigger DNA damage signaling in the absence of DNA lesions (46). However, in our study, we show that the binding of DNA repair factors to nonchromosomal DNA is sufficient to initiate a DNA damage response, since AAV DNA is not associated with histones. This principle is of practical importance, as it may be applied in cancer therapy, where tumor cells could be killed by an indirect induction of a DNA damage response without damaging host DNA.

AAV-induced H2AX phosphorylation is a result of ATR overactivation. The DNA damage signaling pathway activated by AAV is a result of replication stalling on the viral origins of replication (22, 30). This pathway involves ATR, which activates proteins such as Chk1 and leads to an accumulation of DNA repair factors into AAV DNA-containing foci. This study shows that ATR is also needed for the pannuclear phosphorylation of H2AX observed after infection with UV-inactivated AAV. This is in accordance with data from previous studies demonstrating that the γ-H2AX foci induced by stalled replication forks are a result of ATR activation (24, 39, 55). ATM activation, on the other hand, is a result of DNA damage related to double-strand DNA breaks (21). As expected, our data show that ATM is not involved in AAV-induced pannuclear H2AX phosphorylation, since AAV infection does not create double-strand DNA breaks.

How does ATR activation cause pannuclear H2AX phosphorylation? ATR has been shown to colocalize with DNA damage response foci (6, 30), so we considered several possibilities. First, the ATR-containing foci may be mobile and therefore able to phosphorylate H2AX at many sites in the nucleus. However, the results of live-imaging experiments argue against this, because the virus-induced foci were found not to move. Second, ATR, rather than directly phosphorylating H2AX, could activate an effector kinase that diffuses in the nucleus and results in the pannuclear type of H2AX phosphorylation. A candidate for this role is Chk1. When we blocked Chk1 function with the inhibitor UCN01, the level of virus-induced pannuclear H2AX phosphorylation was not reduced (data not shown). Indeed, such inhibition has been reported to promote H2AX phosphorylation by inducing cellular DNA damage (49). Nevertheless, it cannot be excluded that another effector kinase is involved in the H2AX phosphorylation that we observed. Although ATR is clearly located in DNA damage response foci, it is reasonable to assume that the bound ATR is in equilibrium with a certain level of free ATR. We therefore propose, to explain the pannuclear type of H2AX phosphorylation, that AAV infection causes an overactivation of ATR that then diffuses away from the AAV-containing foci and phosphorylates H2AX throughout the nucleus. In another study, activation of ATR has also been shown to lead to a DNA damage response in the absence of cellular DNA breaks (53).

H2AX is dispensable for the formation and maintenance of DNA repair foci. H2AX phosphorylation has been shown to be dispensable for the initial steps of the response induced by DNA double-strand breaks but is required for maintaining the integrity of the induced foci (14). On the other hand, the role of H2AX phosphorylation in the DNA damage response induced by stalled replication forks is still not clear. This study shows that the DNA repair foci induced by aborted replication can be formed and maintained in the absence of H2AX phosphorylation. Phosphorylated RPA, which is an indicator of this kind of DNA damage response, was found to be localized in foci, in the absence of H2AX, even 4 days after the induction of stalled replication signaling by AAV infection. This suggests

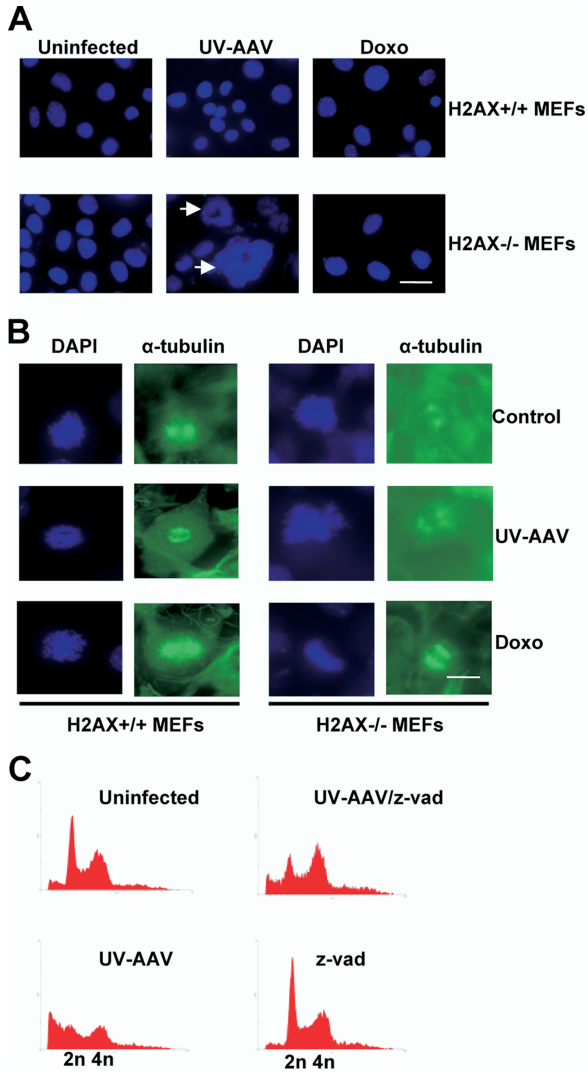

FIG. 8. AAV-infected H2AX$^{-/-}$ cells die of caspase-dependent mitotic catastrophe. (A) The presence of micronucleated cells (indicated by the arrows) was assayed in infected H2AX$^{-/-}$ cells by DAPI staining 4 days after infection. H2AX$^{+/+}$ cells, as well as doxorubicin (Doxo)-treated H2AX$^{-/-}$ cells, did not show signs of mitotic catastrophe. Bar, 30 μm. (B) Defective mitosis was assayed by staining with α-tubulin antibody 4 days postinfection. UV-AAV-infected cells showed multiple spindle poles, whereas H2AX$^{+/+}$ cells and doxorubicin-treated H2AX$^{-/-}$ cells did not. Bar, 12 μm. (C) FACS analysis showing that apoptosis is involved in AAV-mediated killing of H2AX-deficient cells. AAV-infected H2AX$^{-/-}$ cells were treated with the pancaspase inhibitor z-vad (20 μM), which prevented cell death. Treatment with z-vad alone did not have a significant effect on the cells.

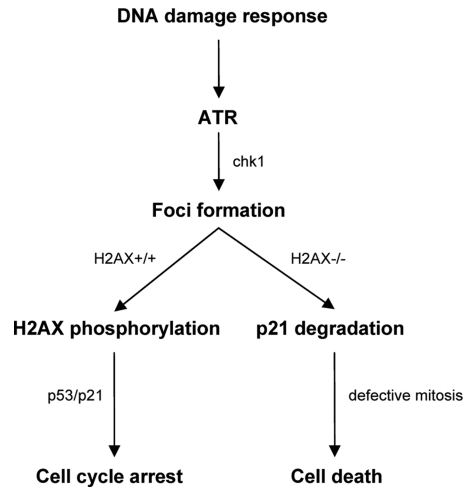

FIG. 9. Model explaining the role of H2AX phosphorylation in the AAV-induced DNA damage response.

that H2AX phosphorylation is a step in the virus-induced DNA damage signaling pathway that is not required for the formation and maintenance of the DNA repair foci. Accumulation of DNA repair factors in foci is one of the immediate results of DNA damage. For this reason, we suggest that H2AX phosphorylation induced by AAV is dispensable for the initial steps of the DNA damage response. This study also shows that H2AX phosphorylation is not required for maintaining the DNA repair foci, in contrast to the DNA double-strand damage situation, where H2AX is essential for this function. Overall, we conclude that H2AX phosphorylation, although massive, is not required for the part of the DNA damage response provoked by AAV stalled replication forks that includes the formation of DNA repair foci and ATR activation. This cellular reaction might, however, be needed for subsequent steps of the DNA damage response.

H2AX is required for p21-induced cell cycle arrest. The response to AAV infection involves an increase in the levels of p53 and p21, which are responsible for subsequent cell cycle arrest. This study shows that in the absence of H2AX, the response to AAV infection is rather different. Infected cells do not arrest but proceed to impaired mitosis that results in cell death. This phenomenon is accompanied by a significant decrease in the levels of p21 that is proteosome dependent. In addition, H2AX seems not to be required for Chk1 activation, since Chk1 levels increased in both H2AX-deficient and -proficient cells. We can therefore conclude that in contrast to ATR and Chk1, H2AX phosphorylation is not required for the DNA damage signaling pathway up to the point where AAV DNA repair foci are formed. Phosphorylated H2AX becomes functional at a later stage, as it is involved in the p53/p21 pathway leading to cell cycle arrest, with the aim of allowing the cell time to resolve the viral DNA problem. In the absence of H2AX phosphorylation cells divert from the p53/p21 pathway and are led to cell death, via defective mitosis, due to the degradation of p21 (Fig. 9). p21 is a known inhibitor of apoptosis, and its degradation can lead to cell death (26, 52). Moreover, it has been shown to inhibit caspase-3, which is a crucial component of apoptotic cell death (48). Several other studies showing that DNA damage-induced p21 degradation leads to cell death also support our model (1, 31).

p21 degradation was not only observed in the DNA damage response induced by AAV. It was also observed in H2AX-deficient cells treated with replication-blocking agents such as HU and UV. This suggests that the role of H2AX in the p53/p21 pathway is important not only in the AAV-induced DNA damage response but also in situations where genomic replication is inhibited. Our data clearly apply to the cellular reaction to replication blocking in general since, despite the

fact that the AAV signal does not come from genomic DNA, the cell activates a DNA damage signaling pathway that is the same as the one induced by genomic stalled replication forks. Finally, the fact that p21-deficient cells die similarly to $H2AX^{-/-}$ cells after AAV infection is another argument supporting our model, which places H2AX in the same pathway as p21 (25, 38).

Cell death in AAV-infected $H2AX^{-/-}$ cells is caused mostly by mitotic catastrophe. This type of cell death is a result of the formation of multiple spindle poles that leads to a defective mitotic process. An absence of p21 has been shown to lead to polyploidy due to the uncoupling of S phase and mitosis and subsequent cell death via apoptosis (54). A recent report has also shown that p21 deficiency leads to centriole overduplication and chromosome instability (18). Although there were no cells with apoptotic appearance in our study, the type of cell death that we observed was caspase dependent, indicating that it might involve an apoptotic pathway. This indicates that these cells die as a result of mitotic defects, leading to caspase-dependent cell death, presumably apoptosis.

Overall, this study reveals a new role of H2AX in the p53/p21 pathway of the DNA damage response induced by stalled replication forks. We show that H2AX is required for increasing p21 levels after replication inhibition and that this subsequently results in checkpoint activation and cell cycle arrest. On the other hand, in the absence of H2AX, cells respond by a p21-independent pathway that leads to apoptosis. The details of how H2AX is involved in the p53/p21 pathway are still unknown; future work should elucidate this. It is possible, based on the known interactions between p21 and PCNA and between PCNA and chromatin, that H2AX phosphorylation interferes with PCNA binding to chromatin, allowing PCNA to bind stably to p21 and preventing its ubiquitination (7). The absence of H2AX phosphorylation may therefore enable PCNA to bind to chromatin and release p21, allowing the ubiquitination and degradation of p21. This would enable the activation of a p21-independent pathway that leads to the cell death that we observed in the H2AX-deficient cells.

ACKNOWLEDGMENTS

We thank Evi Soutoglou, Tony Carr, Andre Nussenzweig, Thomas Melendy, Nicolai Tomilin, Nicole Paduwat, and Maria Choleza for help and materials.

This work was supported by Recherche Suisse contre le Cancer and the Fonds National Suisse de la Recherche Scientifique.

REFERENCES

1. **Allan, L. A., and M. Fried.** 1999. p53-dependent apoptosis or growth arrest induced by different forms of radiation in U2OS cells: p21WAF1/CIP1 repression in UV induced apoptosis. Oncogene **18:**5403–5412.
2. **Amador, V., S. Ge, P. G. Santamaría, D. Guardavaccaro, and M. Pagano.** 2007. APC/C (Cdc20) controls the ubiquitin-mediated degradation of p21 in prometaphase. Mol. Cell **27:**462–473.
3. **Bartek, J., and J. Lukas.** 2001. Mammalian G1- and S-phase checkpoints in response to DNA damage. Curr. Opin. Cell Biol. **13:**738–747.
4. **Bassing, C. H., and F. W. Alt.** 2004. H2AX may function as an anchor to hold broken chromosomal DNA ends in close proximity. Cell Cycle **3:**149–153.
5. **Bassing, C. H., K. F. Chua, J. Sekiguchi, H. Suh, S. R. Whitlow, J. C. Fleming, B. C. Monroe, D. N. Ciccone, C. Yan, K. Vlasakova, D. M. Livingston, D. O. Ferguson, R. Scully, and F. W. Alt.** 2002. Increased ionizing radiation sensitivity and genomic instability in the absence of histone H2AX. Proc. Natl. Acad. Sci. USA **99:**8173–8178.
6. **Bekker-Jensen, S., C. Lukas, R. Kitagawa, F. Melander, M. B. Kastan, J. Bartek, and J. Lukas.** 2006. Spatial organization of the mammalian genome surveillance machinery in response to DNA strand breaks. J. Cell Biol. **173:**195–206.
7. **Bendjennat, M., J. Boulaire, T. Jascur, H. Brickner, V. Barbier, A. Sarasin, A. Fotedar, and R. Fotedar.** 2003. UV irradiation triggers ubiquitin-dependent degradation of p21(WAF1) to promote DNA repair. Cell **114:**599–610.
8. **Berns, K. I.** 1996. *Parvoviridae*: the viruses and their replication, p. 2173–2197. *In* B. N. Fields, D. M. Knipe, P. M. Howley, D. E. Griffin, R. A. Lamb, M. A. Martin, B. Roizman, and S. E. Straus (ed.), Fields virology, 3rd ed. Lippincott-Raven, Philadelphia, PA.
9. **Berthet, C., K. Raj, P. Saudan, and P. Beard.** 2005. How adeno-associated virus Rep78 protein arrests cells completely in S phase. Proc. Natl. Acad. Sci. USA **102:**13634–13639.
10. **Bloom, J., V. Amador, F. Bartolini, G. DeMartino, and M. Pagano.** 2003. Proteasome-mediated degradation of p21 via N-terminal ubiquitinylation. Cell **115:**71–82.
11. **Bunz, F., A. Dutriaux, C. Lengauer, T. Waldman, S. Zhou, J. P. Brown, J. M. Sedivy, K. W. Kinzler, and B. Vogelstein.** 1998. Requirement for p53 and p21 to sustain G2 arrest after DNA damage. Science **282:**1497–1501.
12. **Burdak-Rothkamm, S., S. C. Short, M. Folkard, K. Rothkamm, and K. M. Prise.** 2007. ATR-dependent radiation-induced gamma H2AX foci in bystander primary human astrocytes and glioma cells. Oncogene **26:**993–1002.
13. **Celeste, A., S. Difilippantonio, M. J. Difilippantonio, O. Fernandez-Capetillo, D. R. Pilch, O. A. Sedelnikova, M. Eckhaus, T. Ried, W. M. Bonner, and A. Nussenzweig.** 2003. H2AX haploinsufficiency modifies genomic stability and tumor susceptibility. Cell **114:**371–383.
14. **Celeste, A., O. Fernandez-Capetillo, M. J. Kruhlak, D. R. Pilch, D. W. Staudt, A. Lee, R. F. Bonner, W. M. Bonner, and A. Nussenzweig.** 2003. Histone H2AX phosphorylation is dispensable for the initial recognition of DNA breaks. Nat. Cell Biol. **5:**675–679.
15. **Celeste, A., S. Petersen, P. J. Romanienko, O. Fernandez-Capetillo, H. T. Chen, O. A. Sedelnikova, B. Reina-San-Martin, V. Coppola, E. Meffre, M. J. Difilippantonio, C. Redon, D. R. Pilch, A. Olaru, M. Eckhaus, R. D. Camerini-Otero, L. Tessarollo, F. Livak, K. Manova, W. M. Bonner, M. C. Nussenzweig, and A. Nussenzweig.** 2002. Genomic instability in mice lacking histone H2AX. Science **296:**922–927.
16. **Daniel, R., J. Ramcharan, E. Rogakou, K. D. Taganov, J. G. Greger, W. Bonner, A. Nussenzweig, R. A. Katz, and A. M. Skalka.** 2004. Histone H2AX is phosphorylated at sites of retroviral DNA integration but is dispensable for postintegration repair. J. Biol. Chem. **279:**45810–45814.
17. **Downs, J. A., N. F. Lowndes, and S. P. Jackson.** 2000. A role for Saccharomyces cerevisiae histone H2A in DNA repair. Nature **408:**1001–1004.
18. **Duensing, A., L. Ghanem, R. A. Steinman, Y. Liu, and S. Duensing.** 2006. p21(Waf1/Cip1) deficiency stimulates centriole overduplication. Cell Cycle **5:**2899–2902.
19. **Fernandez-Capetillo, O., A. Celeste, and A. Nussenzweig.** 2003. Focusing on foci: H2AX and the recruitment of DNA-damage response factors. Cell Cycle **2:**426–427.
20. **Fernandez-Capetillo, O., H. T. Chen, A. Celeste, I. Ward, P. J. Romanienko, J. C. Morales, K. Naka, Z. Xia, R. D. Camerini-Otero, N. Motoyama, P. B. Carpenter, W. M. Bonner, J. Chen, and A. Nussenzweig.** 2002. DNA damage-induced G2-M checkpoint activation by histone H2AX and 53BP1. Nat. Cell Biol. **4:**993–997.
21. **Fernandez-Capetillo, O., A. Lee, M. Nussenzweig, and A. Nussenzweig.** 2004. H2AX: the histone guardian of the genome. DNA Repair (Amsterdam) **3:**959–967.
22. **Fragkos, M., M. Breuleux, N. Clément, and P. Beard.** 2008. Recombinant adeno-associated viral vectors are deficient in provoking a DNA damage response. J. Virol. **82:**7379–7387.
23. **Franco, S., M. Gostissa, S. Zha, D. B. Lombard, M. M. Murphy, A. A. Zarrin, C. Yan, S. Tepsuporn, J. C. Morales, M. M. Adams, Z. Lou, C. H. Bassing, J. P. Manis, J. Chen, P. B. Carpenter, and F. W. Alt.** 2006. H2AX prevents DNA breaks from progressing to chromosome breaks and translocations. Mol. Cell **21:**201–214.
24. **Furuta, T., H. Takemura, Z. Y. Liao, G. J. Aune, C. Redon, O. A. Sedelnikova, D. R. Pilch, E. P. Rogakou, A. Celeste, H. T. Chen, A. Nussenzweig, M. I. Aladjem, W. M. Bonner, and Y. Pommier.** 2003. Phosphorylation of histone H2AX and activation of Mre11, Rad50, and Nbs1 in response to replication-dependent DNA double-strand breaks induced by mammalian DNA topoisomerase I cleavage complexes. J. Biol. Chem. **278:**20303–20312.
25. **Garner, E., F. Martinon, J. Tschopp, P. Beard, and K. Raj.** 2007. Cells with defective p53-p21-pRb pathway are susceptible to apoptosis induced by p84N5 via caspase-6. Cancer Res. **67:**7631–7637.
26. **Gartel, A. L., and S. K. Radhakrishnan.** 2005. Lost in transcription: p21 repression, mechanisms, and consequences. Cancer Res. **65:**3980–3985.
27. **Gottifredi, V., K. McKinney, M. V. Poyurovsky, and C. Prives.** 2004. Decreased p21 levels are required for efficient restart of DNA synthesis after S phase block. J. Biol. Chem. **279:**5802–5810.
28. **Harris, S. L., and A. J. Levine.** 2005. The p53 pathway: positive and negative feedback loops. Oncogene **24:**2899–2908.
29. **Jurvansuu, J., M. Fragkos, C. Ingemarsdotter, and P. Beard.** 2007. Chk1 instability is coupled to mitotic cell death of p53-deficient cells in response to virus-induced DNA damage signaling. J. Mol. Biol. **372:**397–406.
30. **Jurvansuu, J., K. Raj, A. Stasiak, and P. Beard.** 2005. Viral transport of DNA damage that mimics a stalled replication fork. J. Virol. **79:**569–580.

31. **Krämer, O. H., S. K. Knauer, D. Zimmermann, R. H. Stauber, and T. Heinzel.** 2008. Histone deacetylase inhibitors and hydroxyurea modulate the cell cycle and cooperatively induce apoptosis. Oncogene **27:**732–740.
32. **Liu, G., and G. Lozano.** 2005. p21 stability: linking chaperones to a cell cycle checkpoint. Cancer Cell **7:**113–114.
33. **Liu, J. S., S. R. Kuo, and T. Melendy.** 2006. DNA damage-induced RPA focalization is independent of gamma-H2AX and RPA hyper-phosphorylation. J. Cell. Biochem. **99:**1452–1462.
34. **Meng, L. H., K. W. Koch, and Y. Pommier.** 2007. Dose-response transition from cell cycle arrest to apoptosis with selective degradation of Mdm2 and p21WAF1/CIP1 in response to the novel anticancer agent, aminoflavone (NSC 686,288). Oncogene **26:**4806–4816.
35. **Moldovan, G. L., B. Pfander, and S. Jentsch.** 2007. PCNA, the maestro of the replication fork. Cell **129:**665–679.
36. **Nghiem, P., P. K. Park, Y. Kim, C. Vaziri, and S. L. Schreiber.** 2001. ATR inhibition selectively sensitizes G1 checkpoint-deficient cells to lethal premature chromatin condensation. Proc. Natl. Acad. Sci. USA **98:**9092–9097.
37. **Paull, T. T., E. P. Rogakou, V. Yamazaki, C. U. Kirchgessner, M. Gellert, and W. M. Bonner.** 2000. A critical role for histone H2AX in recruitment of repair factors to nuclear foci after DNA damage. Curr. Biol. **10:**886–895.
38. **Raj, K., P. Ogston, and P. Beard.** 2001. Virus-mediated killing of cells that lack p53 activity. Nature **412:**914–917.
39. **Rao, V. A., A. M. Fan, L. Meng, C. F. Doe, P. S. North, I. D. Hickson, and Y. Pommier.** 2005. Phosphorylation of BLM, dissociation from topoisomerase IIIα, and colocalization with γ-H2AX after topoisomerase I-induced replication damage. Mol. Cell. Biol. **25:**8925–8937.
40. **Redon, C., D. Pilch, E. Rogakou, O. Sedelnikova, K. Newrock, and W. Bonner.** 2002. Histone H2A variants H2AX and H2AZ. Curr. Opin. Genet. Dev. **12:**162–169.
41. **Rogakou, E. P., C. Boon, C. Redon, and W. M. Bonner.** 1999. Megabase chromatin domains involved in DNA double-strand breaks in vivo. J. Cell Biol. **146:**905–916.
42. **Rogakou, E. P., D. R. Pilch, A. H. Orr, V. S. Ivanova, and W. M. Bonner.** 1998. DNA double-stranded breaks induce histone H2AX phosphorylation on serine 139. J. Biol. Chem. **273:**5858–5868.
43. **Sarkaria, J. N., E. C. Busby, R. S. Tibbetts, P. Roos, Y. Taya, L. M. Karnitz, and R. T. Abraham.** 1999. Inhibition of ATM and ATR kinase activities by the radiosensitizing agent, caffeine. Cancer Res. **59:**4375–4382.
44. **Sheaff, R. J., J. D. Singer, J. Swanger, M. Smitherman, J. M. Roberts, and B. E. Clurman.** 2000. Proteasomal turnover of p21Cip1 does not require p21Cip1 ubiquitination. Mol. Cell **5:**403–410.
45. **Siino, J. S., I. B. Nazarov, M. P. Svetlova, L. V. Solovjeva, R. H. Adamson, I. A. Zalenskaya, P. M. Yau, E. M. Bradbury, and N. V. Tomilin.** 2002. Photobleaching of GFP-labeled H2AX in chromatin: H2AX has low diffusional mobility in the nucleus. Biochem. Biophys. Res. Commun. **297:**1318–1323.
46. **Soutoglou, E., and T. Misteli.** 2008. Activation of the cellular DNA damage response in the absence of DNA lesions. Science **320:**1507–1510.
47. **Suh, E. J., T. Y. Kim, and S. H. Kim.** 2006. PP2Cgamma-mediated S-phase accumulation induced by the proteasome-dependent degradation of p21(WAF1/CIP1). FEBS Lett. **580:**6100–6104.
48. **Suzuki, A., Y. Tsutomi, M. Miura, and K. Akahane.** 1999. Caspase 3 inactivation to suppress Fas-mediated apoptosis: identification of binding domain with p21 and ILP and inactivation machinery by p21. Oncogene **18:**1239–1244.
49. **Syljuåsen, R. G., C. S. Sorensen, L. T. Hansen, K. Fugger, C. Lundin, F. Johansson, T. Helleday, M. Sehested, J. Lukas, and J. Bartek.** 2005. Inhibition of human Chk1 causes increased initiation of DNA replication, phosphorylation of ATR targets, and DNA breakage. Mol. Cell. Biol. **25:**3553–3562.
50. **Taylor, W. R., and G. R. Stark.** 2001. Regulation of the G2/M transition by p53. Oncogene **20:**1803–1815.
51. **Thiriet, C., and J. J. Hayes.** 2005. Chromatin in need of a fix: phosphorylation of H2AX connects chromatin to DNA repair. Mol. Cell **18:**617–622.
52. **Tian, H., E. K. Wittmack, and T. J. Jorgensen.** 2000. p21WAF1/CIP1 antisense therapy radiosensitizes human colon cancer by converting growth arrest to apoptosis. Cancer Res. **60:**679–684.
53. **Toledo, L. I., M. Murga, P. Gutierrez-Martinez, R. Soria, and O. Fernandez-Capetillo.** 2008. ATR signaling can drive cells into senescence in the absence of DNA breaks. Genes Dev. **22:**297–302.
54. **Waldman, T., C. Lengauer, K. W. Kinzler, and B. Vogelstein.** 1996. Uncoupling of S phase and mitosis induced by anticancer agents in cells lacking p21. Nature **381:**713–716.
55. **Ward, I. M., and J. Chen.** 2001. Histone H2AX is phosphorylated in an ATR-dependent manner in response to replicational stress. J. Biol. Chem. **276:**47759–47762.
56. **Winocour, E., M. F. Callaham, and E. Huberman.** 1988. Perturbation of the cell cycle by adeno-associated virus. Virology **167:**393–399.
57. **Xie, Q., J. Hare, J. Turnigan, and M. S. Chapman.** 2004. Large-scale production, purification and crystallization of wild-type adeno-associated virus-2. J. Virol. Methods **122:**17–27.
58. **Ziv, Y., A. Bar-Shira, I. Pecker, P. Russell, T. J. Jorgensen, I. Tsarfati, and Y. Shiloh.** 1997. Recombinant ATM protein complements the cellular A-T phenotype. Oncogene **15:**159–167.